Asian Journal of Chemistry; Vol. 34, No. 7 (2022), 1711-1722

ASIAN JOURNAL OF CHEMISTRY

https://doi.org/10.14233/ajchem.2022.23663

A Fluorescence and Molecular Docking Study on the Interaction of 4′-Hydroxychalcone with Bovine Serum Albumin and Human Serum Albumin

MADHUMITA PATAR, ANKITA JALAN and N. SHAEMNINGWAR MOYON*

Department of Chemistry, National Institute of Technology Silchar, Cachar-788010, India

*Corresponding author: Fax: +91 3842 224797; E-mail: nsmoyon@che.nits.ac.in

Received: 16 November 2021; *Accepted*: 21 February 2022; *Published online*: 15 June 2022; AJC-20845

The interaction of 4′-hydroxychalcone (4′HC) with bovine serum albumin (BSA) and human serum albumin (HSA) was studied under physiological condition (pH=7.0). The fluorescence intensity of both serum albumins was quenched in presence of 4′HC at different temperatures. Stern-Volmer analysis and bimolecular quenching constants indicates the presence of static quenching in BSA. Whereas, fluorescence quenching of HSA is due to both the mechanism of static and dynamic quenching. The formation of ground state complex is further confirmed by absorption spectroscopy. The interaction of 4′HC with BSA is stronger than with HSA. FRET study shows the possible energy transfer between 4′HC with BSA and HSA. The binding site of the protein was identified by molecular docking study. The FTIR and CD analysis indicates conformational change in both the serum albumins. The thermodynamic study indicates that the association of BSA and HSA with 4′HC is spontaneous, enthalpy driver and involves electrostatic force of interaction.

Keywords: 4′-Hydroxychalcone, Bovine serum albumin, Human serum albumin, Fluorescence quenching, Molecular docking.

INTRODUCTION

Chalcones (or 1,3-diaryl-2-propen-1-ones) belong to the polyphenol family and are largely distributed in plants, fruits, and vegetables. They are composed of two aromatic benzene rings connected by a α,β-unsaturated carbonyl group [1,2]. The naturally and synthetically occurring chalcones have numerous therapeutic activities like antifungal, anti-inflammatory, anti-malarial, antimicrobial, antioxidative, antiplatelet, antiviral, anticancer, antibacterial, *etc*. [3-11]. They also serve as precursors for synthesis of flavonoid. Chalcones and its analogues seem to be promising molecular tools to evaluate the change of molecular surroundings both in solution and in biological systems [12-15]. From various studies, it is observed that the antiproliferative property of cancer cell is associated with hydroxyl group present in the chalcone compared to other chalcone derivatives [16]. Additionally, the position of hydroxyl group within the chalcone molecule seems to have a great influence on the activity of the molecule [17-19]. Orlikova *et al.* [16] reported that the hydroxyl group present in the fourth position of the A ring as shown in the scheme is an interesting, safe and promising inhibitor of TNF α-induced NF-κB activation. Although, the interaction between unsubstituted chalcone and BSA has been reported by Naik & Nandibewoor [20], no report on the study of substituted chalcone with protein is available. Moreover, the fact that various activities are associated with derivatives of chalcone containing hydroxyl group makes this study worthwhile.

The most abundant protein found in blood plasma is serum albumins having many physiological functions. They are mainly responsible for the absorption, distribution and metabolism of endogenous and exogenous ligands. It is important to investigate the interaction of drugs with serum albumins at molecular level to understand the drug-protein complex and also draw vital information that can be useful in designing of new drugs with improved therapeutic effectiveness. Both bovine serum albumin (BSA) and human serum albumin (HSA) has 76% resemblance to each other. Also, the bovine serum albumin and human serum albumin possess same homologous domain I, II and III with similar ellipsoidal shape and also accommodate with 17 disulphide bonds. The sudlow site I and sudlow site II present in subdomain IIA and subdomain IIIA of BSA are the major binding sites for aromatic and heterocyclic ligands. The binding site is quite similar in both serum albumins BSA

and HSA, sudlow site I and sudlow site II are also the responsible binding domains for HSA [21,22].

In this work, the interaction of 4′-hydroxychalcone (4′HC) with bovine serum albumin (BSA) and human serum albumin (HSA) was compared by using steady state absorption and fluorescence spectroscopy, FTIR, circular dichroism and molecular docking. The Stern-Volmer quenching constants, binding energies number of binding sites, thermodynamic parameters, nature of binding and the distance between the 4′HC with BSA and HSA were determined. The mechanism of quenching was obtained for both the albumin with 4′HC as well as the possible binding site of the proteins with the drug.

EXPERIMENTAL

Bovine serum albumin (MB083-5G) was purchased from HiMedia. Human serum albumin (A3782-100MG), 4′-hydroxychalcone were obtained from Sigma-Aldrich and used as it is without further purification. Monosodium phosphate and disodium phosphate were obtained from Fisher Scientific. DMSO was obtained Sisco Research Laboratories Pvt. Ltd. and Millipore water was used throughout the experiment.

Sample preparation: The stock solution of BSA and HSA (1×10^{-4} mol L^{-1}) were made using 0.1 M sodium phosphate buffer of pH 7.0. Since 4′HC is sparingly soluble in water, the stock solution of 4′HC (1×10^{-4} mol L^{-1}) was made in Millipore water containing 10% DMSO (v/v). All the working samples were freshly made from the stock solutions. The BSA and HSA concentration was fixed at 3×10^{-6} mol L^{-1} in all the samples and the concentration of 4′HC taken were 0, 2, 4, 6, 8, 10, 12, 16 and 20 ($\times 10^{-6}$ mol L^{-1}), respectively.

Methods: The absorption spectra were recorded by using Cary-bio 100 absorption spectrophotometer in the wavelength range of 200-500 nm. The BSA and HSA concentration was fixed at 3×10^{-6} mol L^{-1} and the concentration of 4′HC was varied from 2×10^{-6} mol L^{-1} to 2×10^{-5} mol L^{-1}.

Fluorescence spectra of BSA and HSA were recorded by Hitachi Model F-4600 spectrofluorimeter equipped with 150W Xenon lamp, a thermostatic cell holder and a thermostat water bath circulatory. The fluorescence was measured at different temperatures using 10 mm quartz cuvette cell. The slit width was fixed at 5 nm both for excitation and emission for BSA whereas slit width was fixed at 5 nm for excitation and 10 nm for emission for HSA and a scan speed of 240 nm per min throughout the experiment. All the emission spectra were scan from 290 nm to 500 nm and corrected for the instrument response function. Fig. 1 shows the absorption spectrum of 4′HC, BSA and HSA, respectively. The absorption intensity of 4′HC shows some overlap at the excitation wavelength (280 nm) and emission wavelength (~340 nm) of BSA and HSA. Therefore, all the fluorescence spectrum of protein was corrected to avoid inner filter effect as described elsewhere using eqn. 1:

$$F_{cor} = F_{obs} \times 10^{(A_1+A_2)/2} \quad (1)$$

where, F_{cor}, F_{obs}, A_1 and A_2 are the corrected fluorescence, fluorescence spectrum of HSA and BSA observed in presence of different concentration of 4′HC, total absorbance of 4′HC at 280 nm and total absorbance of 4′HC at ~340 nm, respectively [23]. The effect of DMSO on the interaction of the drug with HSA and BSA is negligible within the amount used as reported by Papadopoulou *et al.* [24].

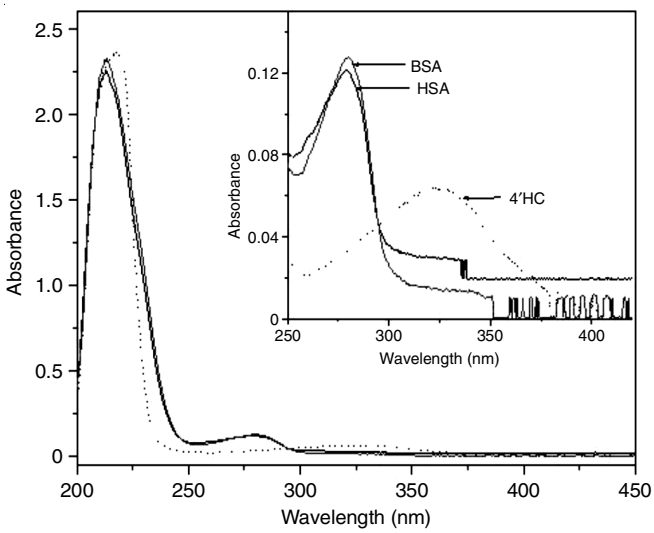

Fig. 1. Absorption spectrum of BSA (3×10^{-6} mol L^{-1}), HSA (3×10^{-6} mol L^{-1}). The dotted line in represents the absorption spectrum of 4′HC (2×10^{-6} mol L^{-1}). Inset shows the zoomed spectra within the range 250-450 nm

FTIR spectra of both HSA and BSA were recorded by using Brukar FTIR spectrometer furnished with a diamond attenuated total reflection (ATR) method in presence and absence of quencher at 298 K in the region 4000-500 cm^{-1}. The concentration of HSA and BSA were fixed at 3×10^{-6} mol L^{-1} and the concentration of 4′HC with both serum albumins is 2×10^{-5} mol L^{-1}.

The circular dichroism spectra were recorded in J-1500 spectropolarimeter in 1 mm path length at 298 K. The spectra were observed wavelength range from 200-250 nm with 50 nm/min scanning speed in 0.5 nm data interval. The concentration of BSA and HSA was fixed 3×10^{-6} mol L^{-1} and the varied ratio of the concentration of 4′HC were 1:1 and 1:3 both for BSA:4′HC and HAS:4′HC, respectively. Phosphate buffer solution pH = 7.0 was used throughout the experiment and the result appeared as an elipticity (mdeg) that is obtained from the instrument directly.

Molecular docking between the optimized structure of 4′HC and the two transport proteins BSA (PDB: 3V03) and HSA (PDB: 1AO6) were performed using Autodock4.2 software downloaded from The Scripps Research Institute (TSRI) [25]. 4′HC was optimized using 6-31G (d,p/B3LYP) level of theory in Gaussian 09 software package [26,27]. Before docking, the proteins were prepared by removing crystallized water molecules and adding polar hydrogens. Later, charges were calculated, all atoms were assigned the AD4 type and saved in PDBQT format. For autogrid calculations of BSA and HSA, the search space dimensions were defined as (120 × 90 × 120) Å with a grid-point spacing of 0.578 Å and (90 × 90 × 100) Å with a grid-point spacing of 0.768 Å, respectively encompassing the entire chain of the proteins. The best docked structure with minimum binding energy was then visualized and further analyzed using PyMol software.

RESULTS AND DISCUSSION

Fluorescence quenching of BSA and HSA with 4′HC: The interaction of BSA and HSA with 4′HC was studied by monitoring the intrinsic BSA and HSA emission in presence of 4′HC. Both BSA and HSA contain fluorescent amino acid residues like tryptophan (Try), tyrosine (Tyr) and phenylalanine (Phe). It is known that when BSA is excited at 295 nm the emission is only from the tryptophan residue whereas, when excited at 280 nm, both Trp and Tyr in the protein are responsible for the emission [28]. However, tyrosine is less fluorescence and as such, the contribution by it is almost negligible. In both the cases, the BSA and HSA emission was measured at different temperatures by exciting at 280 nm. Fig. 2 show the quenching profile of BSA and HSA fluorescence at 298 K in presence of a varied concentration of 4′HC. The fluorescence intensity of both BSA and HSA was found to decrease with an increase in the concentration of 4′HC without any change in the position of emission maxima. A similar trend was observed at higher temperatures 303, 308 and 313 K, respectively in both BSA (Fig. 3) and HSA (Fig. 4). This indicates that there is an interaction in both serum albumins with 4′HC.

Stern-Völmer analysis: The quenching of fluorescence occurs due to various processes like energy transfer, excited state reactions, molecular rearrangement, collision and complex formation in the ground state [29]. Static and dynamic quenching is two most commonly discussed mechanism of fluorescence quenching. Static quenching is due to the formation of a non-fluorescent complex in the ground state whereas, collisional or dynamic quenching occurs due to collision of the excited fluorophore with the same molecules in the ground state or with the quencher. Quenching is well described by Stern-Völmer equation as given below:

$$\frac{F_o}{F} = 1 + K_q \tau_0 [Q] = 1 + K_{SV}[Q] \quad (2)$$

where F and F_o denote the fluorescence intensities of proteins with and without quencher, respectively. K_{SV}, K_q, τ_0 and [Q] are the Stern-Völmer quenching constant, quenching rate constant, decay time of the fluorophore without quencher and the concentration of quencher respectively. Figs. 5 and 6 is the plot of F_0/F *vs.* [Q] at different temperatures 298, 303, 308, 313 K and the corresponding results are given in Table-1.

As can be seen in Figs. 5 and 6, the quenching data were well fitted with Stern-Völmer equation, which indicates that the quenching may be either collisional or static quenching. However, it is well known that static and collisional quenching are dependent on temperature and base on this, the two types

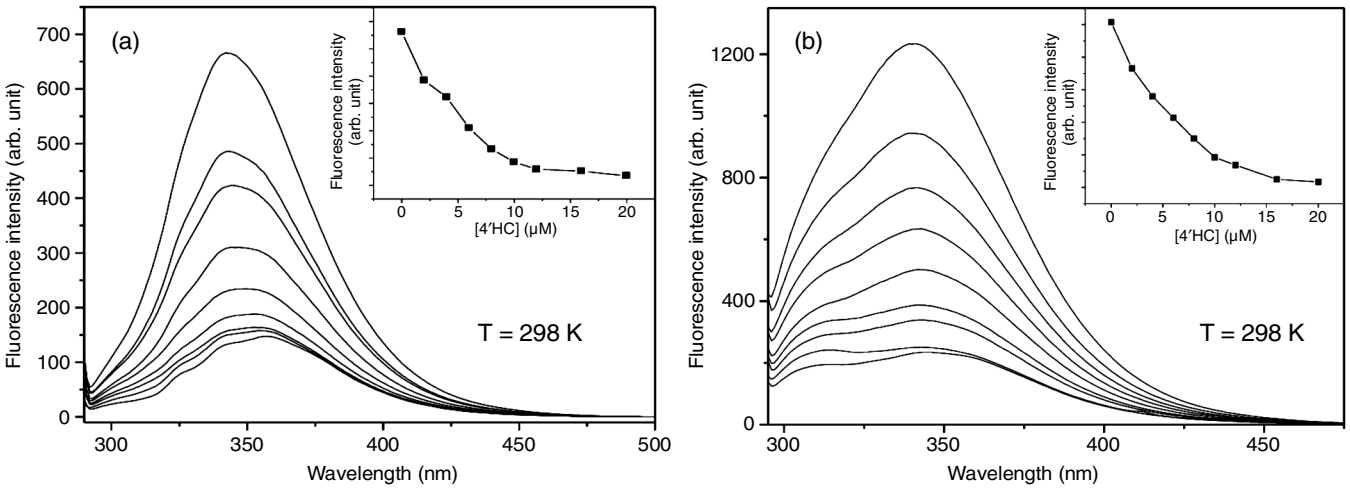

Fig. 2. Fluorescence spectra of (a) BSA and (b) HSA, in different concentrations of 4′HC at 298 K, λ_{exc} = 280 nm; [BSA] and [HSA] = 3 × 10^{-6} mol L^{-1}; [4′HC] = 0, 2, 4, 6, 8, 10, 12, 16, 20 (× 10^{-6} mol L^{-1}). Inset shows the variation of emission intensity with quencher concentration

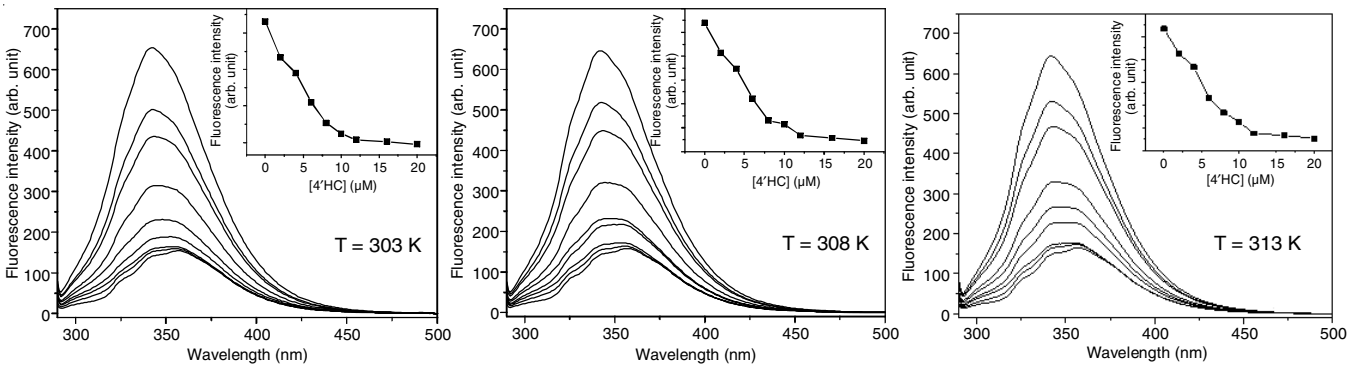

Fig. 3. Fluorescence spectra of BSA in different concentrations of 4′HC at different temperatures, λ_{exc} = 280 nm; [BSA] = 3 × 10^{-6} mol L^{-1}; [4′HC] = 0, 2, 4, 6, 8, 10, 12, 16, 20 (× 10^{-6} mol L^{-1}). Inset shows the variation of emission intensity with quencher concentration

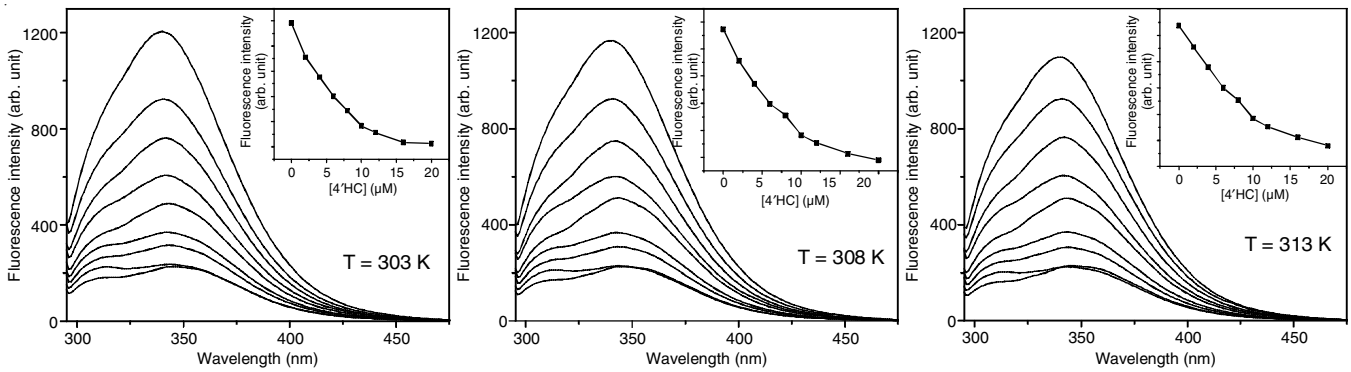

Fig. 4. Fluorescence spectra of HAS in different concentrations of 4′HC at different temperatures, λ_{exc} = 280 nm; [HSA] = 3×10^{-6} mol L^{-1}; [4′HC] = 0, 2, 4, 6, 8, 10, 12, 16, 20 ($\times 10^{-6}$ mol L^{-1}). Inset shows the variation of emission intensity with quencher concentration

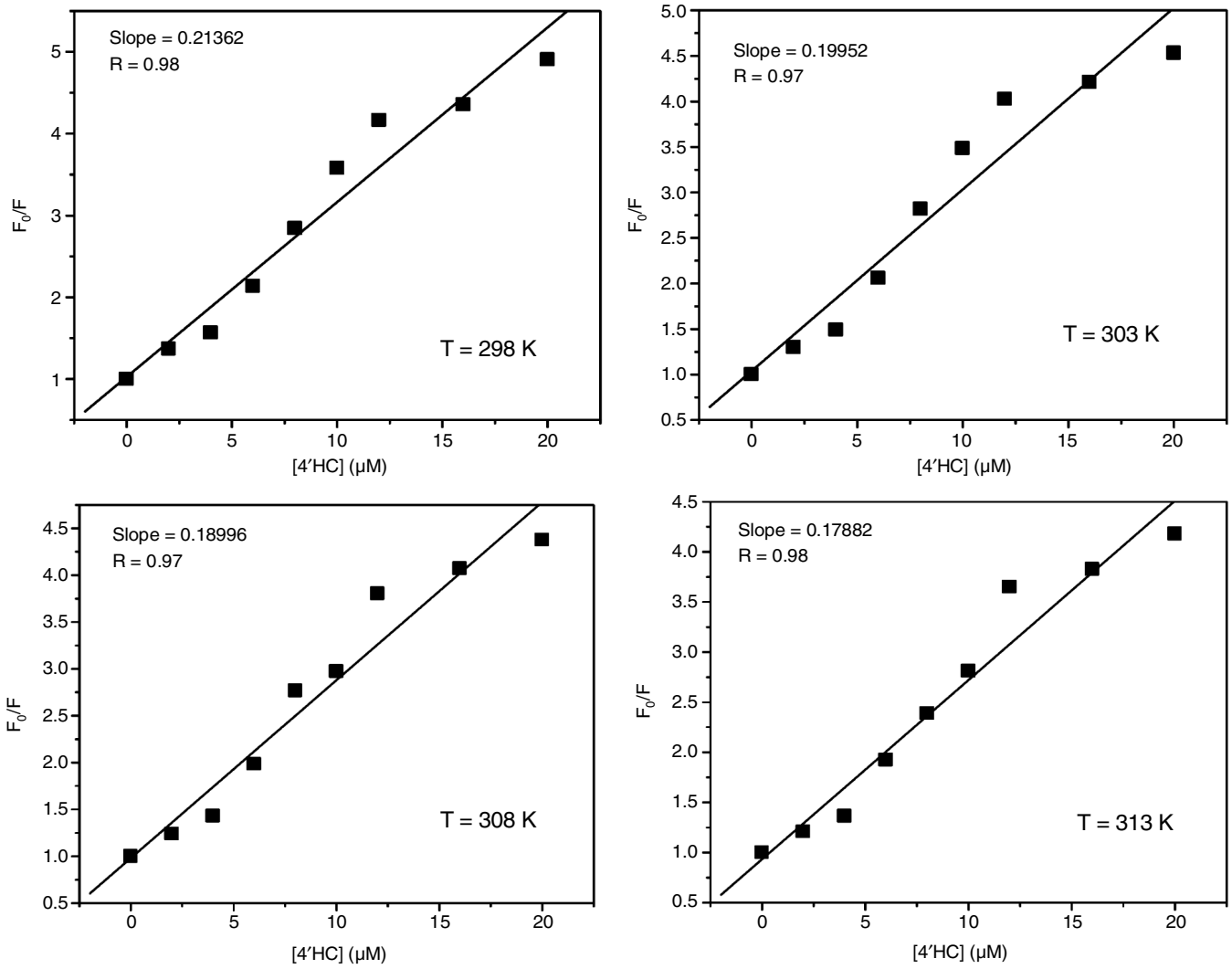

Fig. 5. Stern-Volmer plot for quenching of BSA with 4′HC at different temperatures

TABLE-1
RESULTS OF STERN-VOLMER PLOT OF SERUM ALBUMINS WITH 4′HC AT DIFFERENT TEMPERATURES

Temp. (K)	BSA			HSA		
	K_{SV} ($\times 10^5$ M^{-1})	K_q ($\times 10^{13}$ M^{-1} s^{-1})	R	K_{SV} ($\times 10^5$ M^{-1})	K_q ($\times 10^{13}$ M^{-1} s^{-1})	R
298	2.14	2.14	0.98	2.30	2.30	0.99
303	1.99	1.99	0.97	2.37	2.37	0.97
308	1.89	1.89	0.97	2.76	2.76	0.98
313	1.79	1.79	0.98	2.85	2.85	0.97

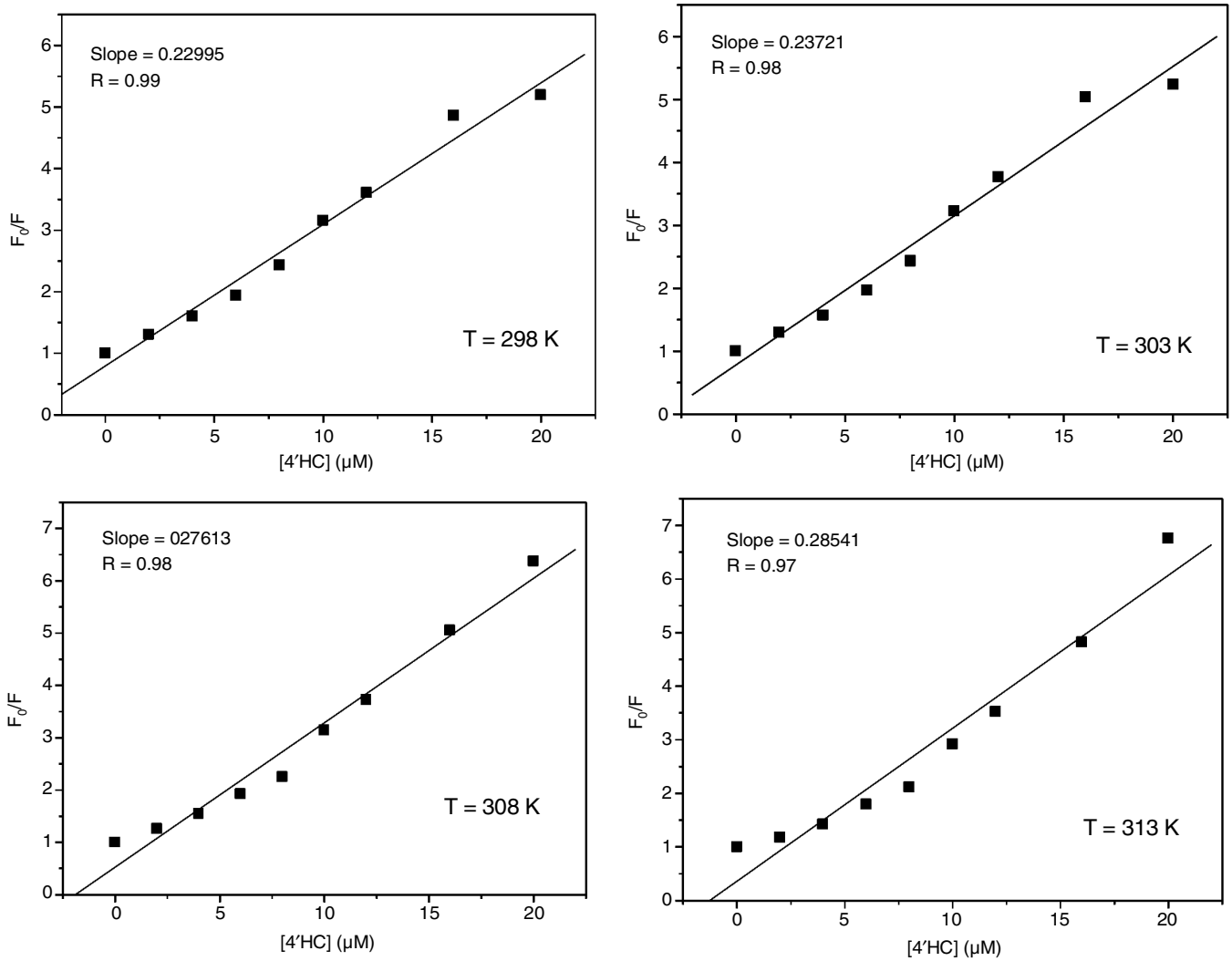

Fig. 6. Stern-Volmer plot for quenching of HSA with 4′HC at different temperatures

of quenching can be distinguished. At higher temperatures, the rate of diffusion would increase and lead to more collisional quenching. In such cases, the Stern-Völmer quenching constant (K_{SV}) will increase with an increase in temperature. Whereas, increase in temperature would increase the dissociation of weakly bound ground state complexes and lead to a decrease in static quenching. Therefore, for static quenching, the K_{SV} will decrease with an increase in temperature and for dynamic quenching, the K_{SV} will increase with an increase in temperature. Table-1 shows that the K_{SV} decreases with an increase in temperature in BSA-4′HC system, which signifies that the quenching of BSA fluorescence by 4′HC is through the formation of ground state BSA-4′HC complexes.

However, the K_{SV} increases with an increase in the temperature indicating that the quenching of HSA fluorescence by 4′HC follows a dynamic quenching mechanism. It is known that the decay time of biopolymer is 10^{-8} s [29-31]. The bimolecular collisional quenching constant (K_q) was calculated from $K_q = K_{SV}/\tau_0$ and is given in Table-1. It is observed that for both BSA and HSA, the K_q values are higher than the maximum collisional quenching constant of various quenchers with the biopolymer (2.0×10^{10} M^{-1} S^{-1}) reported in the literature [32]. This signifies that the mechanism of quenching of both BSA and HSA with 4′HC follows static quenching. However, from the values of both K_a and K_q in the case of HSA-4′HC system, it indicates the presence of both static and dynamic quenching mechanism. This could be due to the interaction of 4′HC with HSA during the incubation time of around 90 min.

Binding constant and number of binding sites: The binding constant (K_a) and the number of binding site (n) can be determined using eqn. 3, which had been successfully employed in the study of many drug-protein interaction to understand the equilibrium between the free and bound molecules [33-36].

$$\log\frac{F_o - F}{F} = n\log K_a + n\log\left([Q] - \frac{F_o - F}{F_o}[P]\right) \quad (3)$$

where, F and F_o denote the fluorescence intensities with and without the quencher, respectively; [Q] is the concentration of quencher and [P] is the protein concentration. The plot of log $\{(F_o\text{-}F)/F\}$ against log $\{[Q]\text{-}[P](F_o\text{-}F)/F\}$ BSA and HSA are given in Figs. 7 and 8, respectively. The binding constant and number of binding sites were determined and displayed in Table-2.

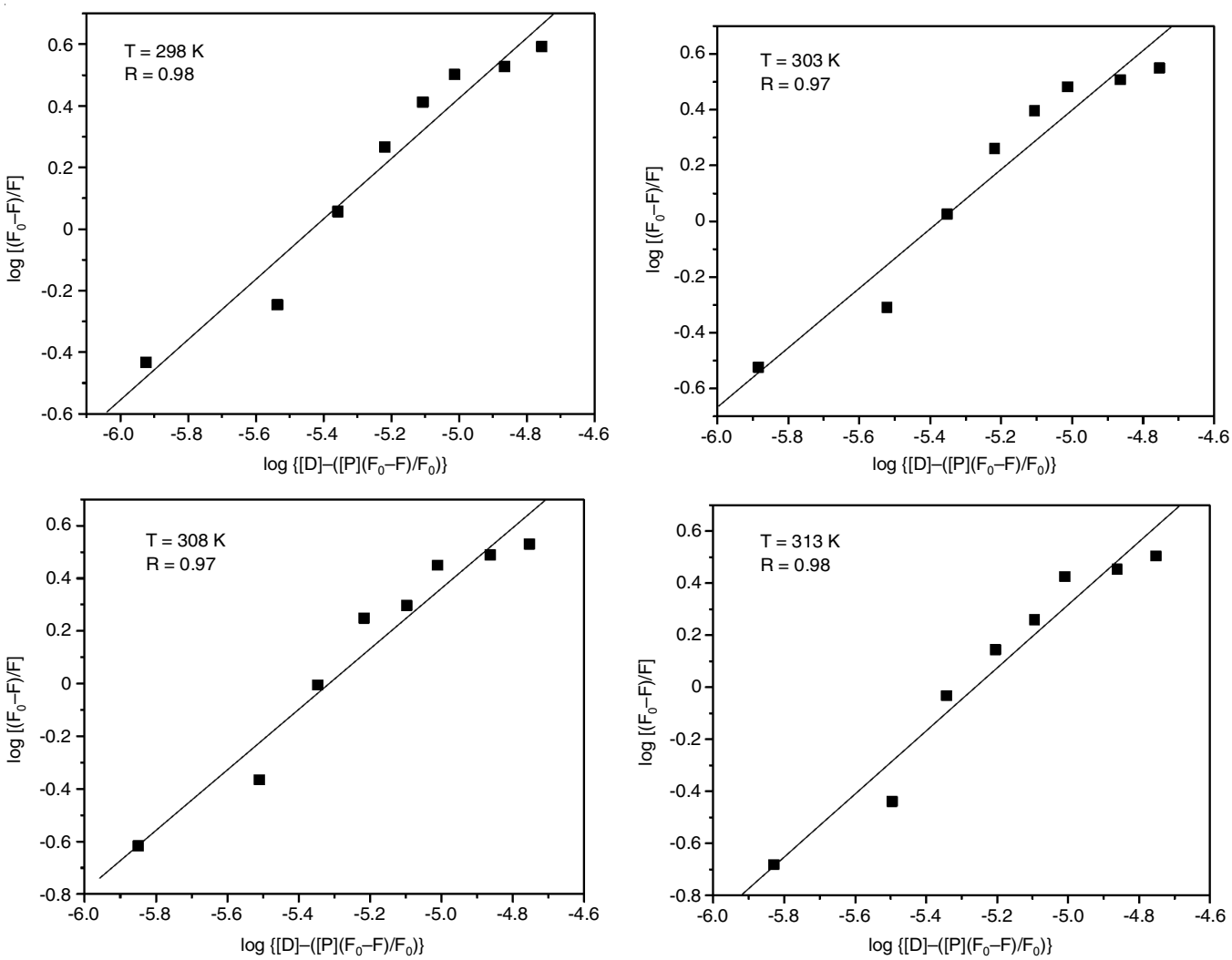

Fig. 7. Plot of log [(F_0-F)/F] against log{[D]-[P](F_0-F)/F} of BSA with 4′HC at different temperatures

TABLE-2
BINDING ENERGY AND NUMBER OF BINDING SITES OBTAINED FROM EQN. 3

Temp. (K)	BSA			HSA		
	K_a ($\times 10^5$ M^{-1})	n	R	K_a ($\times 10^5$ M^{-1})	n	R
298	2.71	0.98	0.98	2.34	1.08	0.99
303	2.37	1.07	0.97	2.33	1.11	0.98
308	2.07	1.15	0.97	2.19	1.24	0.99
313	1.83	1.21	0.98	1.85	1.40	0.99

The decrease in binding constant with an increase in temperature indicates that the stability of BSA-4′HC and HSA-4′HC complexes have reduced as the temperature is increased. The number of binding site 'n' is not significantly altered within the range of temperature considered under study and its value indicates that the 4′HC binds only to one binding site of both BSA and HSA. Higher values of binding constant at lower temperature indicates stronger interaction of 4′HC with BSA than HSA.

Thermodynamic parameters and mode of binding: Various forces account for the interaction of ligands with proteins. These include hydrophobic interaction, electrostatic interaction, van der Waals forces and hydrogen bonding interaction [37]. The force involved can be characterized based on the sign and extent of the thermodynamic parameters like enthalpy change (ΔH) and entropy change (ΔS). If (i) ΔH > 0 and ΔS > 0, the interaction involves hydrophobic interaction; (ii) ΔH < 0 and ΔS > 0, the force is electrostatic interaction; (iii) ΔH < 0 and ΔS < 0, the interaction force is van der Waals force and/or hydrogen bonding interaction [38]. To understand the nature of binding of 4′HC with BSA and HSA, the thermodynamic parameters were calculated by using eqns. 4 and 5.

$$\ln K_a = \frac{\Delta H}{RT} + \frac{\Delta S}{R} \quad (4)$$

$$\Delta G = \Delta H - T\Delta S \quad (5)$$

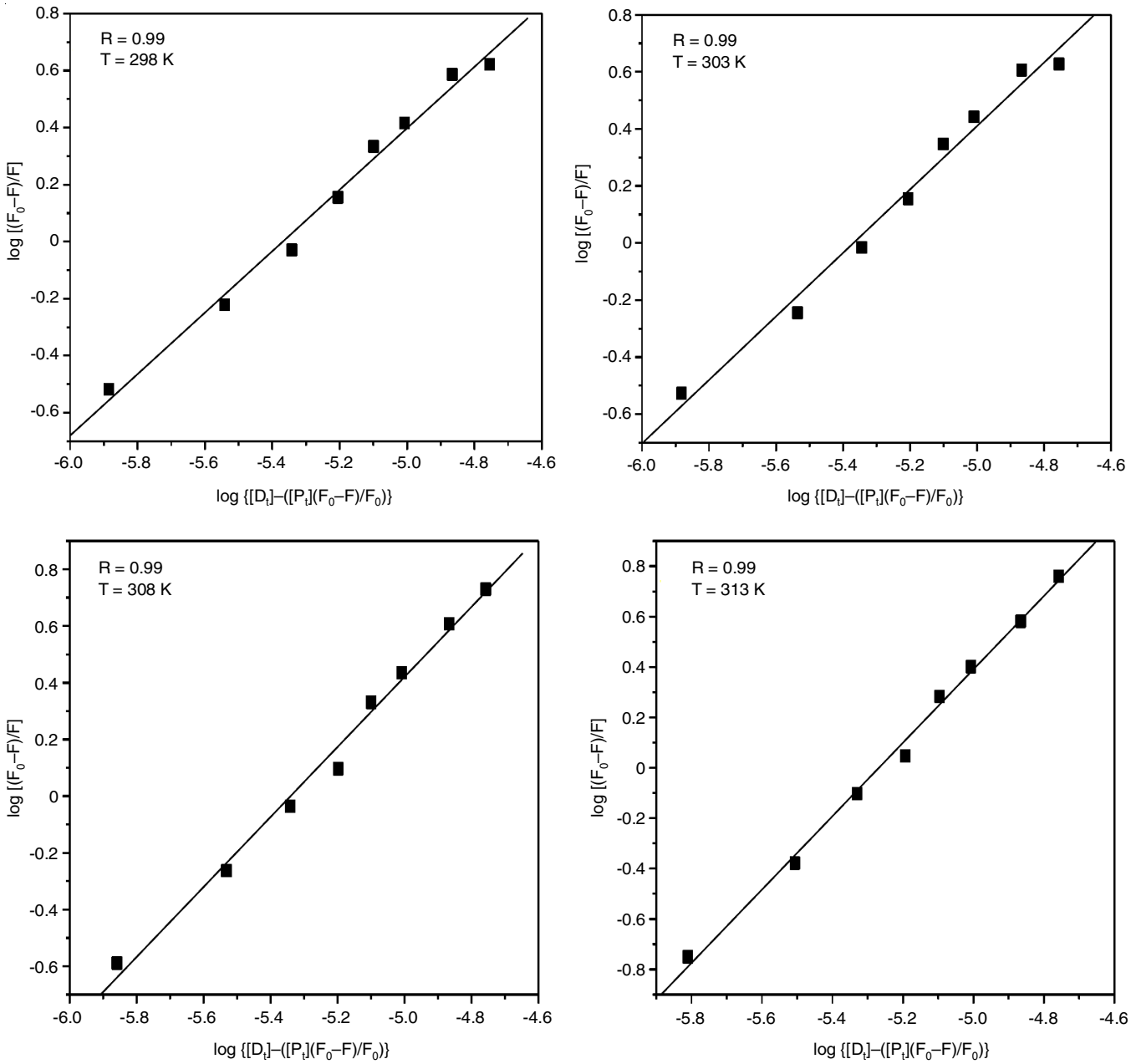

Fig. 8. Plot of log [(F_0-F)/F] against log {[D]-[P](F_0-F)/F} of HSA with 4′HC at different temperatures

where, K_a denotes the associative binding constant of BSA-4′HC and HSA-4′HC complex at a given temperature, R and T denotes the gas constant and the temperature, respectively. Using van't Hoff's plot (Fig. 9), the values of ΔH and ΔS were obtained and subsequently change in Gibbs free energy (ΔG) for all the temperature was calculated using eqn. 5 for both BSA and HSA and are listed in Table-3. Similar nature of interaction was found to be observed in both the proteins. The negative value of ΔG in both the protein-drug systems implies that the binding is found to be spontaneous. The negative value

TABLE-3
BINDING CONSTANTS AND THERMODYNAMIC PARAMETERS OF BSA-4′HC AND HSA-4′HC AT DIFFERENT TEMPERATURES

Temp. (K)	BSA					HSA				
	K_a ($\times 10^5$ mol^{-1})	ΔH (kJ mol^{-1})	ΔS (JK^{-1} mol^{-1})	ΔG (kJ mol^{-1})	R^b	K_a ($\times 10^5$ mol^{-1})	ΔH (kJ mol^{-1})	ΔS (JK^{-1} mol^{-1})	ΔG (kJ mol^{-1})	R^h
298	2.71	-20.59	34.94	-30.99	0.99	2.338	-14.37	55.12	-30.79	0.96
303	2.37			-31.17		2.335			-31.07	
308	2.07			-31.35		2.191			-31.34	
313	1.83			-31.52		1.854			-31.62	

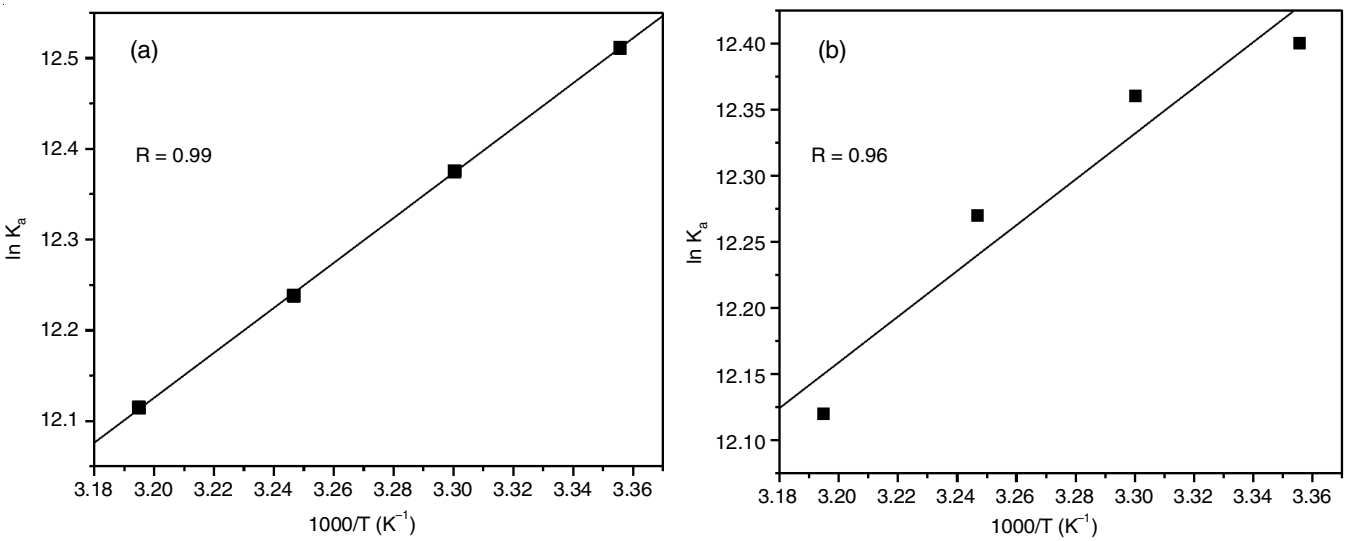

Fig. 9. Van't Hoff plot for binding of 4′HC with (a) BSA (a) and HSA (b)

of ΔH and the positive value of ΔS indicate that 4′HC is bound to both proteins *i.e.* BSA and HSA by the electrostatic force of interaction unlike the hydrophobic interaction of unsubstituted chalcone with BSA as reported by Naik & Nandibewoor [20]. Moreover, the large negative enthalpy change in comparison to positive entropy change shows that the interaction of 4′HC with BSA and HSA is exothermic and mainly driven by enthalpy [39,40].

FRET analysis on the association of serum albumins with 4′HC: The transfer of energy from donor to acceptor is known as Förster resonance energy transfer (FRET). It is widely used in measuring the distance between protein and ligand. The efficiency of energy transfer between protein and the ligand depends on the distance between them, orientation of their respective transition dipole and mainly on the extent of spectral overlap between the fluorescene and absorption spectra of the donor and the acceptor, respectively [41]. Fig. 10 shows the spectral overlap between the donors (BSA, HSA) emission spectrum with that of acceptor (4′HC) absorption spectrum.

According to Förster theory, the energy transfer efficiency (E) is defined by eqn. 6, where, r is the distance between both protein (BSA and HSA) and 4′HC, R_0 represents the Förster critical distance when the efficiency of energy transfer is 50% and was calculated by using eqn. 7.

$$E = 1 - \frac{F}{F_o} = \frac{R_0^6}{R_0^6 + r_0^6} \quad (6)$$

$$R_0^6 = 8.79 \times 10^{-25} K^2 N^4 \Phi J \quad (7)$$

$$J = \frac{\int_0^\infty F(\lambda)\varepsilon(\lambda)\lambda^4 d\lambda}{\int_0^\infty F(\lambda) d\lambda} \quad (8)$$

where, $K^2 = 2/3$ for random orientation in the fluid, N is the average refractive index of the medium in the wavelength range at which there is a remarkable spectral overlap, ϕ is the quantum yield of BSA, HSA and J is the spectral overlap integral between the fluorescence and absorption spectrum of BSA and 4′HC, respectively and was obtained using eqn. 8. where F(λ) is the fluorescence intensity of the donor and ε(λ) is the molar absorption coefficient of the acceptor at wavelength λ. Here, N = 1.335, for BSA and HSA ϕ = 0.15 and 0.118 [41,42],

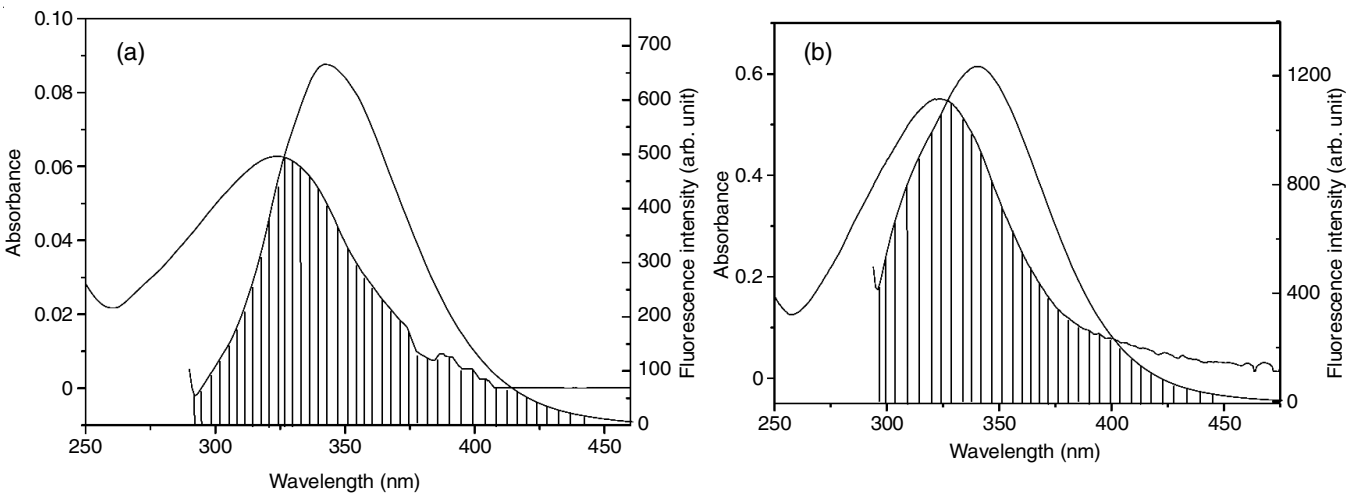

Fig. 10. Spectral overlap of (a) BSA emission and (b) HSA emission with the absorption spectra of 4′HC

respectively. Using eqns. 6-8, $J_{BSA} = 2.482 \times 10^{-14}$ cm^3 LM^{-1}, $J_{HSA} = 2.268 \times 10^{-14}$ cm^3 LM^{-1}, $E_{BSA} = 0.79$, $E_{HSA} = 0.80$, R_0(BSA) = 2.97 nm, R_0(HSA) = 2.81 nm, $r_{BSA} = 2.37$ nm and $r_{HSA} = 2.21$ nm. The binding distance r lies between $0.5R_0$ and $1.5R_0$ indicating that there is a possible energy transfer from BSA and HSA to 4′HC [13].

Analysis of absorption spectra: The absorption spectra of BSA (3×10^{-6} mol L^{-1}) were scanned at different concentration of 4′HC from 250 nm to 370 nm. In Fig. 11, the optical density of BSA and HSA at 280 nm increases with increase in the concentration of 4′HC. In both UV spectra, a small visible shift is observed at 280 nm which might be due to the hyperchromic and bathochromic effects [20,43,44]. This further supports the formation of complex in the ground state.

FTIR studies: According to Naik & Nandibewoor [20], the infrared spectrum showed that the protein contains several amide bands due to different vibrations of the peptide moiety. Amide I of the peptide group is commonly utilized to investigate the change in the protein secondary structure. The amide I and II groups exhibited in the region 1700-1600 cm^{-1} and 1600-1500 cm^{-1}, respectively. However, the amide I is more sensitive even to slightest change in the protein secondary structure thereby making it an appropriate tool for studying the secondary structure of protein [40,45-47]. A close observation of the IR spectrum in Fig. 12, shows that the peak position of amide I shifted from 1643 cm^{-1} to 1636 cm^{-1} and 1639 cm^{-1} to 1637 cm^{-1} in BSA and BSA-4′HC, HSA and HSA-4′HC interaction. This implies that BSA and HSA interact with 4′HC resulting in a change in protein structure and protein micro-environment [44].

Circular dichroism analysis: The circular dichorism spectral observation of BSA and HSA, protein folding spectra mainly indicates two bands at 208 and 222 nm, which corresponds to π–π* and n–π* transitions, respectively [42,47]. The binding of both protein with 4′HC, the disappearance of 208 nm band was observed. But at 222 nm, it was increasing gradually and α-helix % decreases of the proteins. The α-helix % content was calculated at 222 nm by using eqn. 12 [42,47-49].

$$\alpha\text{-Helix}\ (\%) = \left(\frac{(-\text{MRE}_{222} - 2340}{30300}\right) \times 100 \qquad (12)$$

The calculated value of α-helix content in the presence and absence of 4′HC with BSA is 64%, 49% and 38% respectively and for HSA is 47%, 46.8% and 46% respectively. From Fig. 13, it can be seen that the interaction of both proteins with 4′HC led to the disappearance of α-helix band at around 208 nm along with the decrease in the % of α-helix content, which indicates a change in the conformation of the proteins. However, the negligible change in the % of α-helix content in HSA at 222 nm band as compared to BSA suggests that the interaction of 4′HC with both the albumins cause more structural changes in BSA than HSA as reported by Chaves *et al.* [50,51]. This is substantiated by the observations made under IR studies on the interaction of 4′HC with both albumins.

Molecular docking studies: The best energy ranked conformer of 4′HC -BSA and 4′HC -HSA are shown in Fig. 14. In both BSA and HSA, 4′HC interacts in site I in subdomain IIA [52]. The binding free energy change (ΔG) obtained from molecular docking simulation for BSA and HSA were -25.14 kJ mol^{-1} and -25.31 kJ mol^{-1}, respectively which is in fair agreement with the experimentally obtained values (-30.99 and -30.73 kJ mol^{-1}). The residues around 5 Å of 4′HC in site I of BSA are (Fig. 15): PHE-205, ALA-209, ARG-208, ASP-323, ALA-212, LEU-326, GLY-327, LEU-330, LEU-345, LUE-346, ALA-349, LYS-350, VAL-481, ASN-482, SER-479, GLU-478, LEU-480, -NH atom of LEU-480 is hydrogen-bonded with O-atom of 4′HC at a distance of 1.897 Å. Also, the residues in the site I of HSA around 5 Å of 4′HC are (Fig. 16): PHE-206, ALA-210, ALA-213, ARG-209, ASP-324, GLY-328, LEU-481, VAL-482, SER-480, GLU-479, ASN-483, LEU-347, LEU-346, ASN-483, LYS-351, GLU-354, ALA-350. The –NH atom of LEU-481 of HSA (chain A) is

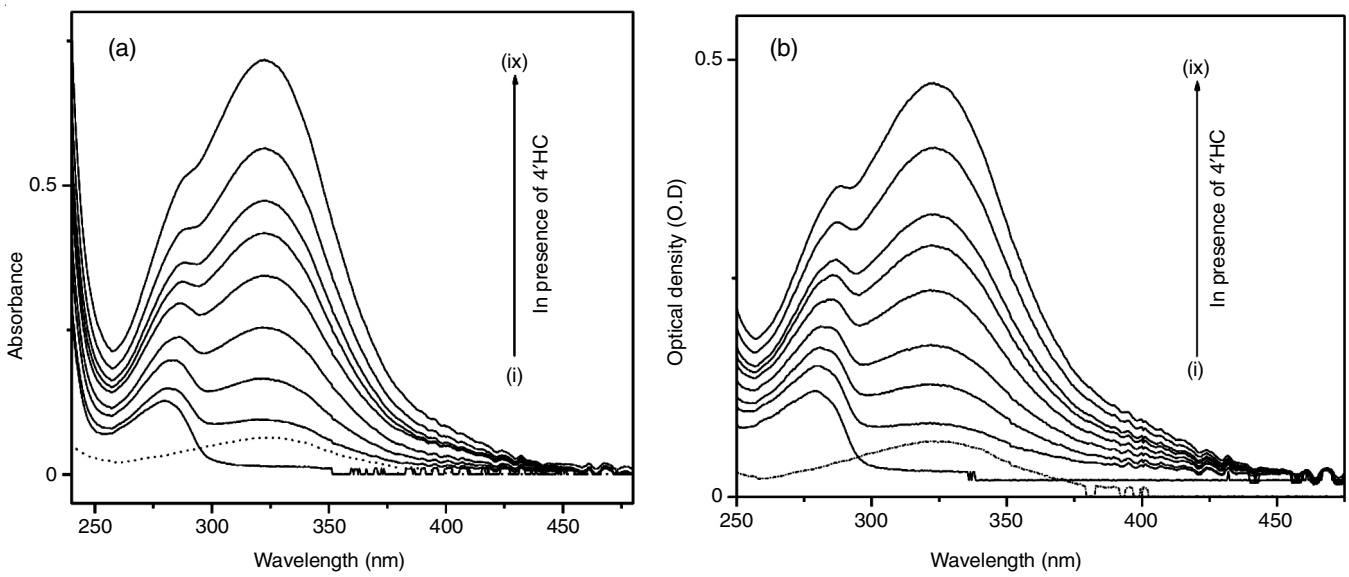

Fig. 11. Absorbance spectra (a) 4′HC (dot lines) and 4′HC–BSA (solid line), (b) 4′HC (dash dot line) and 4′HC–HSA (solid line). [BSA] = [HSA] = 3×10^{-6} mol L^{-1}, [4′HC] = (i) 0 (ii) 2, (iii) 4, (iv) 6, (v) 8, (vi) 10, (vii) 12, (viii) 16, (ix) 20 ($\times 10^{-6}$ mol L^{-1})

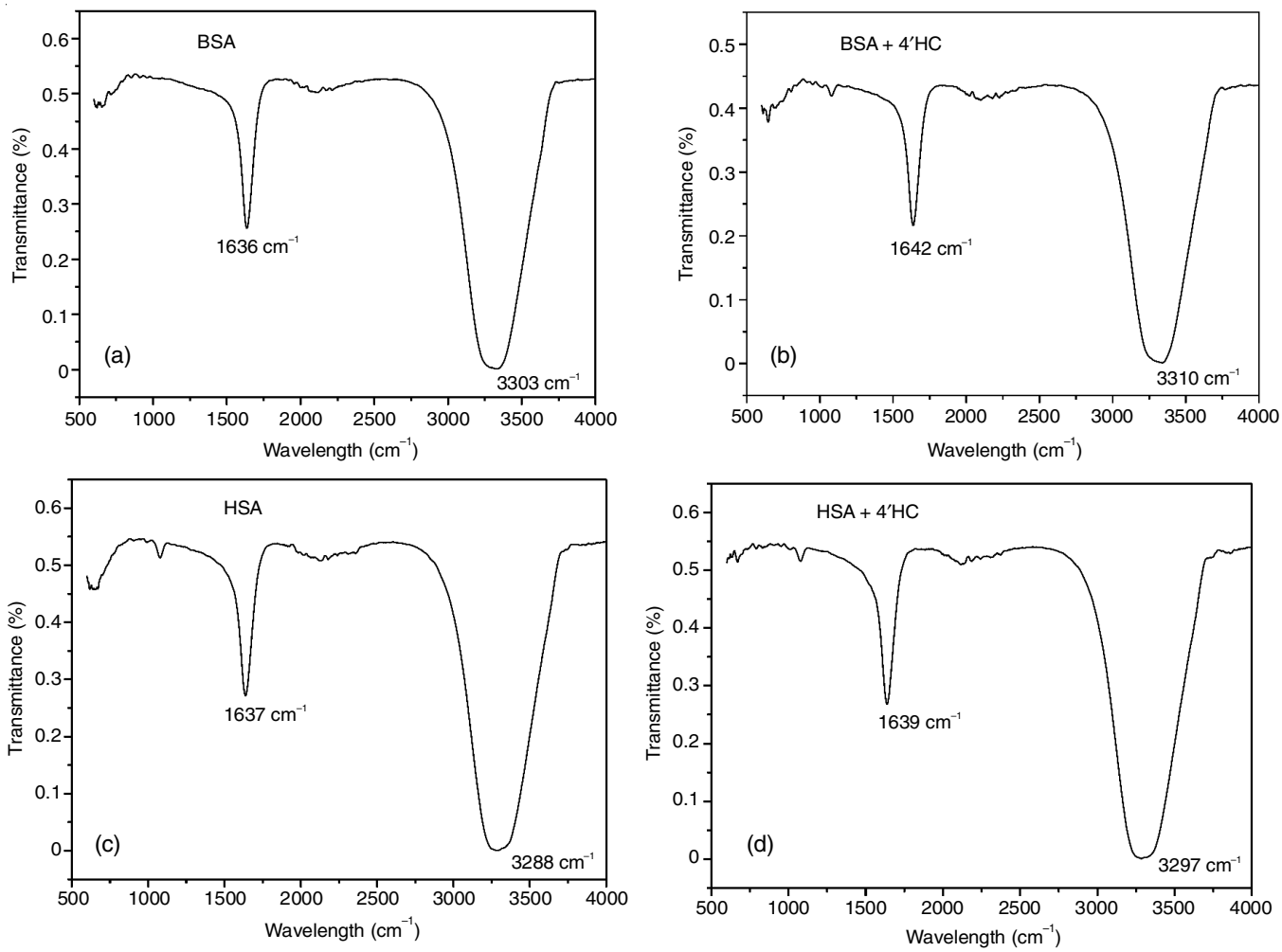

Fig. 12. FTIR spectra of (a) BSA, (b) BSA- 4′HC, (c) HSA and (d) HSA-4′HC

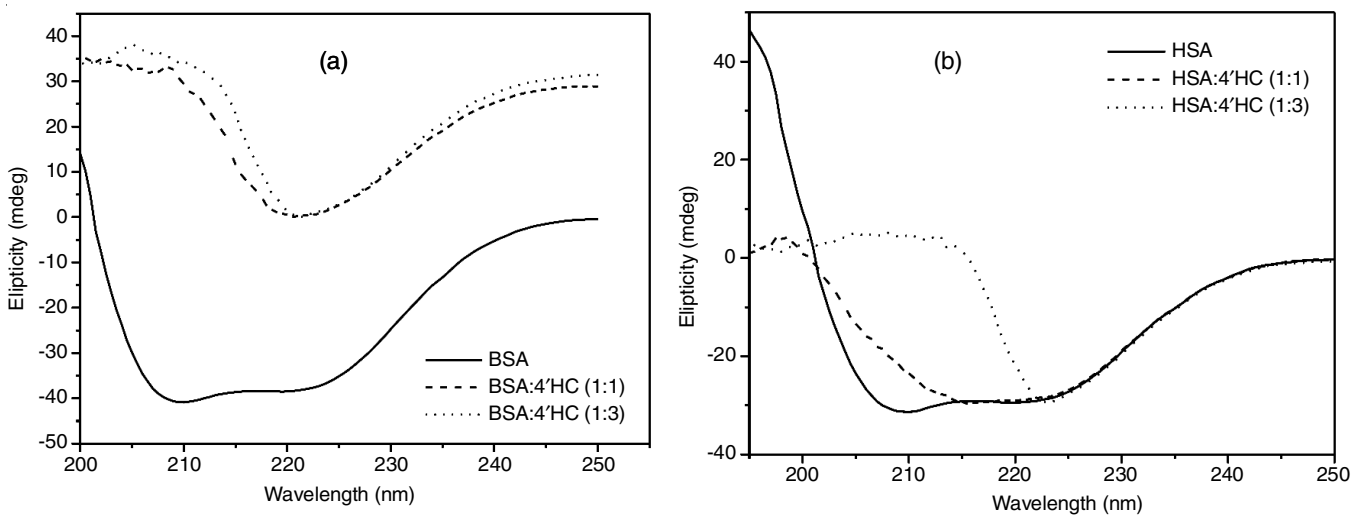

Fig. 13. Circular Dichroism spectra of BSA-4′HC (a) and HSA-4′HC (b)

hydrogen-bonded with O-atom of 4′HC at a distance of 2.08 Å. These results provided a good structural basis at a molecular level to understand the binding of 4′HC with serum albumins, it suggests that 4′HC interacts with serum albumins and hence it provides firm support to the fluorescence quenching results obtained experimentally.

Conclusion

In this work, the interaction of 4′-hydroxychalcone (4′HC) with bovine serum albumin (BSA) and human serum albumin (HSA) was studied using steady-state absorption and fluorescence, FTIR, circular dichroism and molecular docking. Both BSA and HSA fluorescence spectra were found to quenched

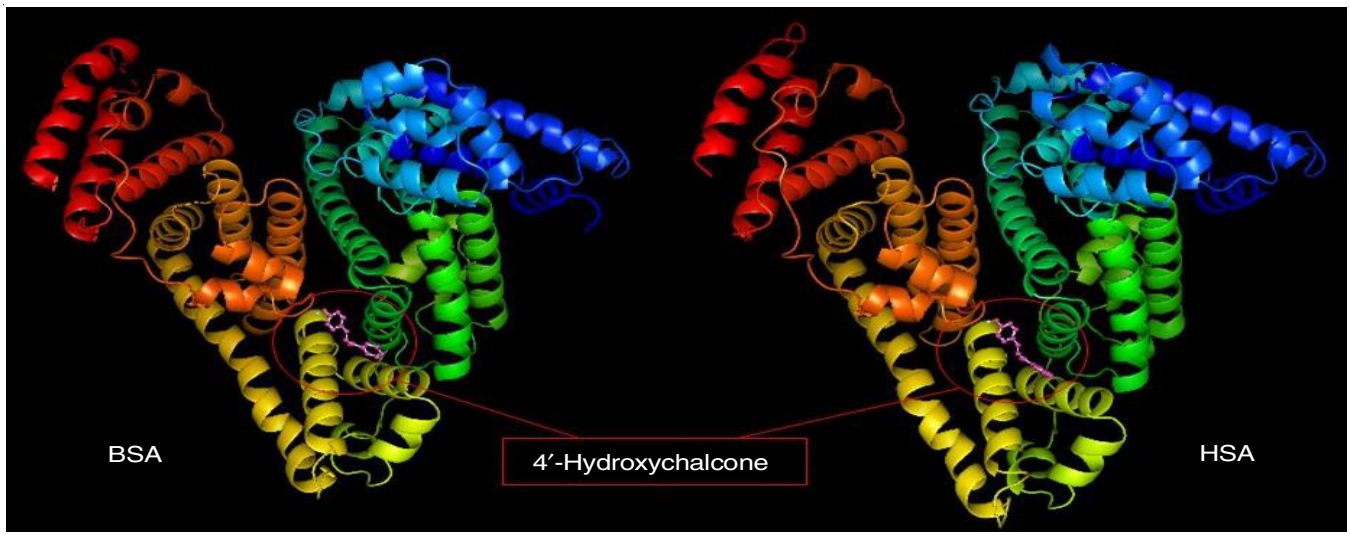

Fig. 14. Molecular docking analysis of 2HF-BSA interactions. The best dock conformation of 2HF-BSA with the lowest energy

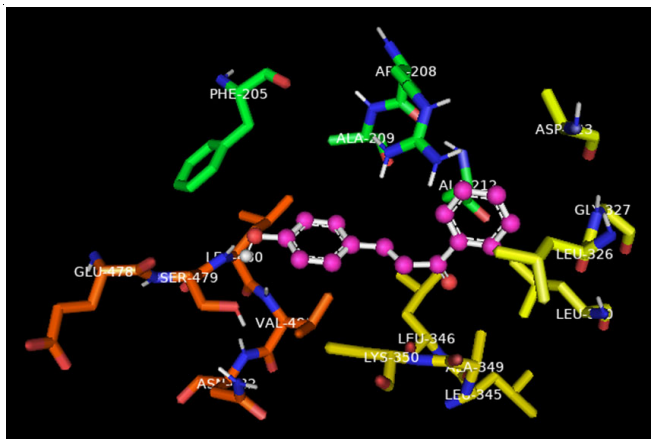

Fig. 15. Amino acid residues of BSA around 5 Å of 4′HC

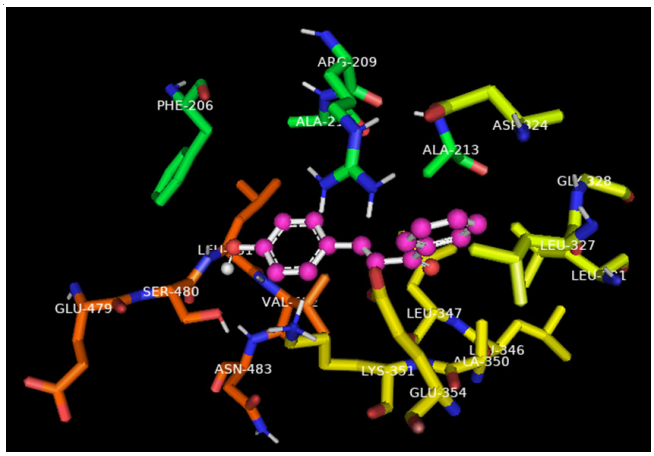

Fig. 16. Amino acid residues of HSA around 5 Å of 4′HC

in presence of different concentrations of 4′HC at different temperatures. Stern-Völmer analysis of the quenching data indicates that the mechanism of quenching for BSA is static quenching and in case of HSA is dynamic quenching. However, the calculated value of bimolecular quenching constant which is higher than the maximum bimolecular collisional quenching constant for both albumin supports the static quenching observed in BSA-4′HC system and suggest the involvement of static dynamic quenching in HSA-4′HC interaction. The formation of 4′HC complexes with BSA and HSA in the ground state is further confirmed from absorption spectroscopy. The value of *n* shows the availability of only one binding site in both the proteins. Molecular docking studies indicate that 4′HC binds to the sub-domain IIA of both the proteins. The Förster distance 'r' for both BSA-4′HC and HSA-4′HC systems lie within $0.5R_0$ and $1.5R_0$, which indicates the possible energy transfer between the protein and ligand. The negative ΔG indicates that the 4′HC-BSA and 4′HC-HSA interaction is spontaneous. The negative ΔH and positive ΔS indicates that the forces involved in the formation of both the complexes is the electrostatic force of interaction. FTIR and CD studies show some conformation changes both in BSA and HSA after the interaction with 4′HC.

ACKNOWLEDGEMENTS

Sincere gratitude to National Institute of Technology Silchar, Assam, India, for providing financial assistance. Also thankful to Advance Material Research Centre (AMRC), IIT Mandi, India for circular dichroism spectra.

CONFLICT OF INTEREST

The authors declare that there is no conflict of interests regarding the publication of this article.

REFERENCES

1. Y. Xue, Y. Zheng, L. An, L. Zhang, Y. Qian, D. Yu, X. Gong and Y. Liu, *Comput. Theor. Chem.*, **982**, 74 (2012); https://doi.org/10.1016/j.comptc.2011.12.020
2. D.K. Mahapatra, V. Asati and S.K. Bharti, *Eur. J. Med. Chem.*, **92**, 839 (2015); https://doi.org/10.1016/j.ejmech.2015.01.051
3. M.S. Özaslan, Y. Demir, H.E. Aslan, S. Beydemir and Ö.I. Küfrevioglu, *J. Biochem. Mol. Toxicol.*, **32**, e22047 (2018); https://doi.org/10.1002/jbt.22047
4. K.L. Lahtchev, D.I. Batovska, S.P. Parushev, V.M. Ubiyvovk and A.A. Sibirny, *Eur. J. Med. Chem.*, **43**, 2220 (2008); https://doi.org/10.1016/j.ejmech.2007.12.027
5. Z. Nowakowska, *Eur. J. Med. Chem.*, **42**, 125 (2007); https://doi.org/10.1016/j.ejmech.2006.09.019

6. M. Liu, P. Wilairat, S.L. Croft, A.L.-C. Tan and M.-L. Go, *Bioorg. Med. Chem.*, **11**, 2729 (2003); https://doi.org/10.1016/S0968-0896(03)00233-5
7. Z. Nowakowska, B. Kedzia and G. Schroeder, *Eur. J. Med. Chem.*, **43**, 707 (2008); https://doi.org/10.1016/j.ejmech.2007.05.006
8. S. Vogel, S. Ohmayer, G. Brunner and J. Heilmann, *Bioorg. Med. Chem.*, **16**, 4286 (2008); https://doi.org/10.1016/j.bmc.2008.02.079
9. L.-M. Zhao, H.-S. Jin, L.-P. Sun, H.-R. Piao and Z.-S. Quan, *Bioorg. Med. Chem. Lett.*, **15**, 5027 (2005); https://doi.org/10.1016/j.bmcl.2005.08.039
10. Z. Wan, D. Hu, P. Li, D. Xie and X. Gan, *Molecules*, **20**, 11861 (2015); https://doi.org/10.3390/molecules200711861
11. L. Ni, C.Q. Meng and J.A. Sikorski, *Expert Opin. Ther. Pat.*, **14**, 1669 (2004); https://doi.org/10.1517/13543776.14.12.1669
12. V. Tomeckova, M. Poskrobova, M. Stefanisinova and P. Perjesi, *Spectrochim. Acta A Mol. Biomol. Spectrosc.*, **74**, 1242 (2009); https://doi.org/10.1016/j.saa.2009.09.048
13. M. Cabrera, M. Simoens, G. Falchi, M.L. Lavaggi, O.E. Piro, E.E. Castellano, A. Vidal, A. Azqueta, A. Monge, A.L. de Ceráin, G. Sagrera, G. Seoane, H. Cerecetto and M. González, *Bioorg. Med. Chem.*, **15**, 3356 (2007); https://doi.org/10.1016/j.bmc.2007.03.031
14. T.A. Fayed and M.K. Awad, *Chem. Phys.*, **303**, 317 (2004); https://doi.org/10.1016/j.chemphys.2004.06.023
15. K. Fodor, V. Tomescova, T. Koszegi, I. Kron and P. Perjesi, *Monatsh. Chem.*, **142**, 463 (2011); https://doi.org/10.1007/s00706-011-0463-0
16. B. Orlikova, D. Tasdemir, F. Golais, M. Dicato and M. Diederich, *Biochem. Pharmacol.*, **82**, 620 (2011); https://doi.org/10.1016/j.bcp.2011.06.012
17. R.C. Bargou, F. Emmerich, D. Krappmann, K. Bommert, M.Y. Mapara, W. Arnold, H.D. Royer, E. Grinstein, A. Greiner, C. Scheidereit and B. Dörken, *J. Clin. Invest.*, **100**, 2961 (1997); https://doi.org/10.1172/JCI119849
18. J. Loa, P. Chow and K. Zhang, *Cancer Chemother. Pharmacol.*, **63**, 1007 (2009); https://doi.org/10.1007/s00280-008-0802-y
19. K.S. Ahn, G. Sethi and B.B. Aggarwal, *Biochem. Pharmacol.*, **75**, 907 (2008); https://doi.org/10.1016/j.bcp.2007.10.010
20. K.M. Naik and S.T. Nandibewoor, *J. Lumin.*, **143**, 484 (2013); https://doi.org/10.1016/j.jlumin.2013.05.013
21. A. Szkudlarek, D. Pentak, A. Ploch, J. Pozycka and M. Maciazek-Jurczyk, *Molecules*, **22**, 569 (2017); https://doi.org/10.3390/molecules22040569
22. I.R. Singh and S. Mitra, *Spectrochim. Acta A Mol. Biomol. Spectrosc.*, **206**, 569 (2019); https://doi.org/10.1016/j.saa.2018.08.055
23. L. Khalili and G. Dehghan, *J. Lumin.*, **211**, 193 (2019); https://doi.org/10.1016/j.jlumin.2019.03.048
24. A. Papadopoulou, R.J. Green and R.A. Frazier, *J. Agric. Food Chem.*, **53**, 158 (2005); https://doi.org/10.1021/jf048693g
25. G.M. Morris, D.S. Goodsell, R.S. Halliday, R. Huey, W.E. Hart, R.K. Belew and A.J. Olson, AutoDock, Version 4.0.1, The Scripps Research Institute, La Jolla, CA, USA (2007).
26. Y. Zhao and D.G. Truhlar, *Acc. Chem. Res.*, **41**, 157 (2008); https://doi.org/10.1021/ar700111a
27. M.J. Frisch, G.W. Trucks, H.B. Schlegel, G.E. Scuseria, M.A. Robb, J.R. Cheeseman, G. Scalmani, V. Barone, B. Mennucci, G.A. Petersson, H. Nakatsuji, M. Caricato, X. Li, H.P. Hratchian, A.F. Izmaylov, J. Bloino, G. Zheng, J.L. Sonnenberg, M. Hada, M. Ehara, K. Toyota, R. Fukuda, J. Hasegawa, M. Ishida, T. Nakajima, Y. Honda, O. Kitao, H. Nakai, T. Vreven, J.A. Montgomery, Jr., J.E. Peralta, F. Ogliaro, M. Bearpark, J.J. Heyd, E. Brothers, K.N. Kudin, V.N. Staroverov, R. Kobayashi, J. Normand, K. Raghavachari, A. Rendell, J.C. Burant, S. S. Iyengar, J. Tomasi, M. Cossi, N. Rega, J.M. Millam, M. Klene, J.E. Knox, J.B. Cross, V. Bakken, C. Adamo, J. Jaramillo, R. Gomperts, R.E. Stratmann, O. Yazyev, A.J. Austin, R. Cammi, C. Pomelli, J.W. Ochterski, R.L. Martin, K. Morokuma, V.G. Zakrzewski, G.A. Voth, P. Salvador, J.J. Dannenberg, S. Dapprich, A.D. Daniels, Ö. Farkas, J.B. Foresman, J.V. Ortiz, J. Cioslowski and D.J. Fox, Gaussian 09, Revision A.02, Gaussian, Inc., Wallingford CT (2009).
28. O.A. Chaves, V.A. da Silva, C.M.R. Sant'Anna, A.B.B. Ferreira, T.A.N. Ribeiro, M.G. de Carvalho, D. Cesarin-Sobrinho and J.C. Netto-Ferreira, *J. Mol. Struct.*, **1128**, 606 (2017); https://doi.org/10.1016/j.molstruc.2016.09.036
29. J.R. Lankowicz, Principles of Fluorescence Spectroscopy, Springer Science + Business Media: NY, Ed.: 3 (2006).
30. J.R. Lakowicz and G. Weber, *Biochemistry*, **12**, 21 (1973).
31. Y.Z. Zhang, J. Dai, X. Xiang, W.W. Li and Y. Liu, *Mol. Biol. Rep.*, **37**, 1541 (2010); https://doi.org/10.1007/s11033-009-9555-x
32. J. Xiao, J. Shi, H. Cao, S. Wu, F. Ren and M. Xu, *J. Pharm. Biomed. Anal.*, **45**, 609 (2007); https://doi.org/10.1016/j.jpba.2007.08.032
33. P. Mandal and T. Ganguly, *J. Phys. Chem. B*, **113**, 14904 (2009); https://doi.org/10.1021/jp9062115
34. X. Yan, B. Liu, B. Chong and S. Cao, *J. Lumin.*, **142**, 155 (2013); https://doi.org/10.1016/j.jlumin.2013.04.009
35. G. Zhang, N. Zhao, X. Hu and J. Tian, *Spectrochim. Acta A Mol. Biomol. Spectrosc.*, **76**, 410 (2010); https://doi.org/10.1016/j.saa.2010.04.009
36. H. Hamishehkar, S. Hosseini, A. Naseri, A. Safarnejad and F. Rasoulzadeh, *Bioimpacts*, **6**, 125 (2016); https://doi.org/10.15171/bi.2016.19
37. P.D. Ross and S. Subramanian, *Biochemistry*, **20**, 3096 (1981); https://doi.org/10.1021/bi00514a017
38. A. Jahanban-Esfahlan and V. Panahi-Azar, *Food Chem.*, **202**, 426 (2016); https://doi.org/10.1016/j.foodchem.2016.02.026
39. T.A. Wani, H. AlRabiah, A.H. Bakheit, M.A. Kalam and S. Zargar, *Chem. Cent. J.*, **11**, 134 (2017); https://doi.org/10.1186/s13065-017-0366-1
40. M.S. Ali and H.A. Al-Lohedan, *J. Mol. Liq.*, **278**, 385 (2019); https://doi.org/10.1016/j.molliq.2019.01.034
41. V.D. Suryawanshi, L.S. Walekar, A.H. Gore, P.V. Anbhule and G.B. Kolekar, *J. Pharm. Anal.*, **6**, 56 (2016); https://doi.org/10.1016/j.jpha.2015.07.001
42. A. Khammari, A.A. Saboury, M.H. Karimi-Jafari, M. Khoobi, A. Ghasemi, S. Yousefinejad and O.K. Abou-Zied, *Phys. Chem. Chem. Phys.*, **19**, 10099 (2017); https://doi.org/10.1039/C7CP00681K
43. O.A. Chaves, D. Cesarin-Sobrinho, C.M.R. Sant'Anna, M.G. de Carvalho, L.R. Suzart, F.E.A. Catunda-Junior, J.C. Netto-Ferreira and A.B.B. Ferreira, *J. Photochem. Photobiol. Chem.*, **336**, 32 (2017); https://doi.org/10.1016/j.jphotochem.2016.12.015
44. J. Ma, Y. Fan, Q. Si, Y. Liu, X. Wang, H. Liu and M. Xie, *Anal. Sci.*, **33**, 493 (2017); https://doi.org/10.2116/analsci.33.493
45. S.-Y. Lin, Y.-S. Wei, M.-J. Li and S.-L. Wang, *Eur. J. Pharm. Biopharm.*, **57**, 457 (2004); https://doi.org/10.1016/j.ejpb.2004.02.005
46. K. Rahmelow and W. Hubner, *Anal. Biochem.*, **241**, 5 (1996); https://doi.org/10.1006/abio.1996.0369
47. N. Singh, N. Kumar, G. Rathee, D. Sood, A. Singh, V. Tomar, S.K. Dass and R. Chandra, *ACS Omega*, **5**, 2267 (2020); https://doi.org/10.1021/acsomega.9b03479
48. H. Kumar, V. Devaraji, R. Joshi, M.K. Jadhao, P. Ahirkar, R. Prasath, P. Bhavana and S.K. Ghosh, *RSC Adv.*, **5**, 65496 (2015); https://doi.org/10.1039/C5RA08778C
49. M.F. AlAjmi, M.T. Rehman, R.A. Khan, M.A. Khan, G. Muteeb, M.S. Khan, O.M. Noman, A. Alsalme and A. Hussain, *Spectrochim. Acta A Mol. Biomol. Spectrosc.*, **225**, 117457 (2020); https://doi.org/10.1016/j.saa.2019.117457
50. O.A. Chaves, L.S. de Barros, M.C.C. de Oliveira, C.M.R. Sant'Anna, A.B.B. Ferreira, F.A. da Silva, D. Cesarin-Sobrinho and J.C. Netto-Ferreira, *J. Fluor. Chem.*, **199**, 30 (2017); https://doi.org/10.1016/j.jfluchem.2017.04.007
51. O.A. Chaves, B. Mathew, D. Cesarin-Sobrinho, B. Lakshminarayanan, M. Joy, G.E. Mathew, J. Suresh and J.C. Netto-Ferreira, *J. Mol. Liq.*, **242**, 1018 (2017); https://doi.org/10.1016/j.molliq.2017.07.091
52. X. Zhang, L. Li, Z. Xu, Z. Liang, J. Su, J. Huang and B. Li, *PLoS One*, **8**, e59106 (2013); https://doi.org/10.1371/journal.pone.0059106